

# Consistent Treatment of Propagator Modifications in Elastic Nucleon-Nucleus Scattering within the Spectator Expansion

C.R. Chinn<sup>(a),(b)</sup>, Ch. Elster<sup>(c)</sup>, R.M. Thaler<sup>(a),(d)</sup>, and S.P. Weppner<sup>(c)</sup>.

<sup>(a)</sup> *Department of Physics and Astronomy, Vanderbilt University, Nashville, TN 37235*

<sup>(b)</sup> *Center for Computationally Intensive Physics, Oak Ridge National Laboratory,  
Oak Ridge, TN 37831*

<sup>(c)</sup> *Institute of Nuclear and Particle Physics, and Department of Physics,  
Ohio University, Athens, OH 45701*

<sup>(d)</sup> *Physics Department, Case Western Reserve University, Cleveland, OH 44106.*

(February 9, 2008)

## Abstract

The theory of the elastic scattering of a nucleon from a nucleus is presented in the form of a Spectator Expansion of the optical potential. Particular attention is paid to the treatment of the free projectile – nucleus propagator when the coupling of the struck target nucleon to the residual target must be taken into consideration. First order calculations within this framework are shown for neutron total cross-sections and for proton scattering for a number of target nuclides at a variety of energies. The calculated values of these observables are in very good agreement with measurement.

PACS: 25.40.Cm, 25.40Dn, 24.10.Ht

Typeset using REVTeX

## I. INTRODUCTION

The theoretical approach to the elastic scattering of a nucleon from a nucleus, pioneered by Watson [1], made familiar by Kerman, McManus, and Thaler (KMT) [2] and further developed as the Spectator Expansion [3–5] is now being applied with striking success. In a similar vein, a slightly different approach to the multiple scattering expansion within the KMT framework is being pursued by the Surrey group [6].

The theoretical motivation for the Spectator Expansion derives from our present inability to calculate the full many-body problem. In this case an expansion is constructed within a consistent multiple scattering theory predicated upon the idea that two-body interactions between the projectile and the target nucleons inside the nucleus play the dominant role. In the Spectator Expansion the first order term involves two-body interactions between the projectile and one of the target nucleons, the second order term involves the projectile interacting with two target nucleons and so forth. Hence the expansion derives the ordering from the number of target nucleons interacting directly with the projectile, while the residual target nucleus remains ‘passive’. Due to the many-body nature of the free propagator for the projectile + target system it is necessary to detail certain choices made with respect to the ordering in the Spectator series. Presented in this paper are the details of the Spectator Expansion and the present manner in which the first order theory is calculated, including a theoretical treatment of the many-body propagator as affected by the residual target nucleus. Predictions are shown for rigorous calculations of the elastic scattering of protons and neutrons from a variety of target nuclei in the energy regime between 65 and 400 MeV. The calculated observables are in very good agreement with the experimental information within this energy regime, indicating the success that this theory enjoys. It is very satisfying to observe in this completely consistent theoretical framework, that as the sophistication of the calculation is increased, the resulting predictions invariably improve.

The calculation of the multiple scattering theory as presented in this paper relies on two basic inputs. One is the fully off-shell nucleon-nucleon (NN) t-matrix, which represents

the best current understanding of the nuclear force, and the other is the nuclear wave function of the target, representing the best present understanding of the ground state of the target nucleus. These quantities comprise the required physical ingredients for a microscopic construction of an optical potential for elastic scattering. To account for the modifications of the free propagator inside the nucleus, mean field potentials taken from microscopic nuclear structure calculations are used. It must be emphasized that there are no adjustable parameters present in these calculations.

The motivation for ongoing work on this topic is twofold. First, elastic and inelastic nucleon-nucleus scattering provide an important and sensitive test for theoretical corrections at the first-order level of the optical potential (*e.g.* as given by possibly genuine modifications of the NN interaction in the nuclear environment and off-shell effects). Rigorous microscopic calculations are required for discerning these effects. A clear understanding of this theory is also necessary before steps can be taken to address the next level of sophistication. Second, a better understanding of the theoretical details of the optical potential are needed to construct realistic and physically sound wave functions representing continuum nucleons in the interior of the nucleus. These wave functions will become vital for future theoretical needs in high-energy coincidence experiments at CEBAF, inelastic scattering studies, and for understanding the reactions in heavy ion experiments involving the new generation of radioactive beam facilities. (In one sense to be able to develop a microscopic scattering theory for heavy ions it is necessary to first clarify the multiple scattering theory of hadronic probes.)

The theoretical framework is presented in Section II, namely the Spectator Expansion, the first order term, the modification of the propagator due to the residual spectator nucleons and the second order term. Section III provides the details of the calculations and the results for neutron-nucleus and proton-nucleus elastic scattering. A conclusion follows in Section IV.

## II. THEORETICAL FRAMEWORK

### A. The Spectator Expansion

The basic motivation behind the Spectator Expansion is that the solution of the full many-body problem is beyond present capabilities, hence an expansion series is constructed for multiple scattering theory predicated upon the number of target nucleons interacting directly with the projectile. Hence the expansion involves terms where the projectile interacts directly with one target nucleon plus a second order term where the projectile interacts directly with two target nucleons, and so on to third and subsequent orders. The separation of these terms with respect to these categories of interactions is not completely fixed due to the nature of the complicated  $A + 1$  body propagator, hence some possible choices detailed in this paper must be differentiated.

At the heart of the standard approach to the elastic scattering of a single projectile from a target of  $A$  particles is the separation into two parts of the Lippmann-Schwinger equation for the transition operator  $T$ , as given by

$$T = V + VG_0(E)T. \quad (2.1)$$

These two parts are an integral equation for  $T$ ,

$$T = U + UG_0(E)PT, \quad (2.2)$$

where here  $U$  is the optical potential operator, and an integral equation for  $U$

$$U = V + VG_0(E)QU. \quad (2.3)$$

In the above equations the operator  $V$  represents the external interaction, such that the Hamiltonian for the entire  $A + 1$  particle system is given by

$$H = H_0 + V. \quad (2.4)$$

Asymptotically the system is in an eigenstate of  $H_0$ , and the free propagator  $G_0(E)$  for the projectile + target nucleus system is

$$G_0(E) = (E - H_0 + i\varepsilon)^{-1}. \quad (2.5)$$

The operators  $P$  and  $Q$  are projection operators,  $P + Q = 1$  and  $P$  is defined such that Eq. (2.2) is solvable. In this case  $P$  is conveniently taken to project onto the elastic channel, such that, among other properties we have

$$[G_0, P] = 0. \quad (2.6)$$

For the scattering of a single particle projectile from an  $A$ -particle target the free Hamiltonian is given by

$$H_0 = h_0 + H_A, \quad (2.7)$$

where  $h_0$  is the kinetic energy operator for the projectile and  $H_A$  stands for the target Hamiltonian. Thus the projector  $P$  can be defined as

$$P = \frac{|\Phi_A\rangle\langle\Phi_A|}{\langle\Phi_A|\Phi_A\rangle}, \quad (2.8)$$

where  $|\Phi_A\rangle$  corresponds to the ground state of the target, satisfying the condition given in Eq. (2.6), and fulfilling

$$H_A|\Phi_A\rangle = E_A|\Phi_A\rangle. \quad (2.9)$$

With these definitions the transition operator for elastic scattering may be defined as  $T_{el} = PTP$ , in which case Eq. (2.2) can be written as

$$T_{el} = PUP + PUPG_0(E)T_{el}. \quad (2.10)$$

Thus, the transition operator for elastic scattering is given by a straightforward one-body integral equation, which requires, of course, the knowledge of the operator  $PUP$ . The theoretical treatment which follows consists of a formulation of the many-body equation, Eq. (2.3), where expressions for  $U$  are derived such that  $PUP$  can be calculated accurately without having to solve the complete many-body problem.

For the present discussion, the presence of two-body forces only is assumed. The extension to  $A$ -body forces is straightforward. With this assumption the operator  $U$  for the optical potential can be expressed as

$$U = \sum_{i=1}^A U_i \quad (2.11)$$

where  $U_i$  is given by

$$U_i = v_{0i} + v_{0i}G_0(E)Q \sum_{j=1}^A U_j, \quad (2.12)$$

provided that

$$V = \sum_{i=1}^A v_{0i}. \quad (2.13)$$

The two-body potential,  $v_{0i}$ , acts between the projectile and the  $i$ th target nucleon. Through the introduction of an operator  $\tau_i$  which satisfies

$$\tau_i = v_{0i} + v_{0i}G_0(E)Q\tau_i, \quad (2.14)$$

Eq. (2.12) can be rearranged as

$$U_i = \tau_i + \tau_i G_0(E)Q \sum_{j \neq i} U_j. \quad (2.15)$$

This rearrangement process can be continued for all  $A$  target particles, so that the operator for the optical potential can be expanded in a series of  $A$  terms of the form

$$U = \sum_{i=1}^A \tau_i + \sum_{i,j \neq i}^A \tau_{ij} + \sum_{i,j \neq i, k \neq i,j}^A \tau_{ijk} + \cdots. \quad (2.16)$$

This is the Spectator Expansion, where each term is treated in turn. The separation of the interactions according to the number of interacting nucleons has a certain latitude, due to the many-body nature of  $G_0(E)$ .

We now concentrate on  $\tau_{ij}$ , which appears in the second term of Eq. (2.16). Its ingredients are readily obtained from Eq. (2.12) by means of the definition

$$(U_i - \tau_i) \equiv \sum_{j \neq i} \xi_{ij}. \quad (2.17)$$

The operator  $\xi_{ij}$ , so defined, satisfies the following many-body integral equation

$$\begin{aligned}
\xi_{ij} &= \tau_i G_0(E) Q \tau_j + \sum_{k \neq j} \tau_i G_0(E) Q \xi_{jk} \\
&= \tau_i G_0(E) Q \tau_j + \tau_i G_0(E) Q \xi_{ji} + \tau_i G_0(E) Q \sum_{k \neq i, j} \xi_{jk} \\
&= \tau_i G_0(E) Q \tau_j + \tau_i G_0(E) Q \xi_{ji} + O(i, j, k).
\end{aligned} \tag{2.18}$$

Omitting all (i,j,k) terms on the right hand side of Eq. (2.18) leads to the second term in Eq. (2.16) via the identification of  $\tau_{ij}$  as

$$\tau_{ij} = \tau_i G_0(E) Q \tau_j + \tau_i G_0(E) Q \tau_{ji}. \tag{2.19}$$

The physical interpretation of Eq. (2.19) can be most easily recognized through an operator  $\chi_{ij}$ , defined as

$$\chi_{ij} = \tau_i + \tau_{ij}, \tag{2.20}$$

from which the following relation is obtained:

$$\chi_{ij} = \tau_i + \tau_i G_0(E) Q \chi_{ji}. \tag{2.21}$$

From the symmetric combination,  $\tilde{U}_{ij} \equiv \chi_{ij} + \chi_{ji}$ , a standard three-body equation is derived:

$$\tilde{U}_{ij} = (v_{0i} + v_{0j}) + (v_{0i} + v_{0j}) G_0(E) Q \tilde{U}_{ij}. \tag{2.22}$$

The finite series given in Eq (2.16) together with the definitions of  $\tau_i$ ,  $\tau_{ij}$ ,  $\dots$  given above constitute one form of the Spectator Expansion in multiple scattering theory. Various other forms could also be found [4]. Differences between one form or another reside primarily in the treatment of the many-body propagator  $G_0(E)$ . The Spectator Expansion derives its name from the underlying idea that in lowest order all target constituents but the initially struck one (particle  $i$ ) are ‘passive’. In the next order all target constituents but the  $i$ th and  $j$ th particle are passive, and so on. In that sense, the Spectator Expansion resembles the linked-cluster decomposition of nuclear structure [7].

## B. The First Order Term

The first order term in the Spectator Expansion,  $\tau_i$  as given by Eq. (2.14), is now examined. Since for elastic scattering only  $P\tau_i P$ , or equivalently  $\langle \Phi_A | \tau_i | \Phi_A \rangle$  need be considered, Eq. (2.14) can be reexpressed with this in mind as

$$\begin{aligned}\tau_i &= v_{0i} + v_{0i}G_0(E)\tau_i - v_{0i}G_0(E)P\tau_i \\ &= \hat{\tau}_i - \hat{\tau}_i G_0(E)P\tau_i,\end{aligned}\tag{2.23}$$

or

$$\langle \Phi_A | \tau_i | \Phi_A \rangle = \langle \Phi_A | \hat{\tau}_i | \Phi_A \rangle - \langle \Phi_A | \hat{\tau}_i | \Phi_A \rangle \frac{1}{(E - E_A) - h_0 + i\varepsilon} \langle \Phi_A | \tau_i | \Phi_A \rangle,\tag{2.24}$$

where  $\hat{\tau}_i$  is defined as the solution of

$$\hat{\tau}_i = v_{0i} + v_{0i}G_0(E)\hat{\tau}_i.\tag{2.25}$$

The combination of Eqs. (2.23) and (2.2) corresponds to the first order Watson scattering expansion [1]. If the projectile – target nucleon interaction is assumed to be the same for all target nucleons and if isospin effects are neglected then the KMT scattering integral equation [2] can be derived from the first order Watson scattering expansion.

Since Eq. (2.24) is a simple one-body integral equation, the principal problem is to find a solution of Eq. (2.25). Of course, due to the many-body character of  $G_0(E)$ , Eq. (2.25) is a many-body integral equation, and in fact no more easily solved than the original equation Eq. (2.1). However,  $G_0(E)$  may be written as

$$\begin{aligned}G_0(E) &= (E - h_0 - H_A + i\varepsilon)^{-1} \\ &= (E - h_0 - h_i - W_i - H^i + i\varepsilon)^{-1}\end{aligned}\tag{2.26}$$

with

$$W_i = \sum_{j \neq i} V_{ij}\tag{2.27}$$

and

$$H^i = H_A - h_i - W_i. \quad (2.28)$$

Since  $H^i$  has no explicit dependence on the  $i$ th particle, then Eq. (2.25) may be simplified by the replacement of  $H^i$  by an average energy  $E^i$ . This is not necessarily an approximation since  $G_0(E)$  might be regarded to be

$$G_0(E) = [(E - E^i) - h_0 - h_i - W_i - (H^i - E^i) + i\varepsilon]^{-1} \quad (2.29)$$

and  $(H^i - E^i)$  could be set aside to be treated in the next order of the expansion of the propagator  $G_0(E)$ . Thus, consider now  $G_0(E)$  to be  $G_i(E)$ , where

$$G_i(E) = [(E - E^i) - h_0 - h_i - W_i + i\varepsilon]^{-1}, \quad (2.30)$$

so that  $\hat{\tau}_i = \tilde{\tau}_i + (\text{higher order corrections})$ , and Eq. (2.25) reduces to

$$\tilde{\tau}_i = v_{0i} + v_{0i}G_i(E)\tilde{\tau}_i. \quad (2.31)$$

Eq. (2.31) can also be reexpressed as

$$\tilde{\tau}_i = t_{0i} + t_{0i}g_iW_iG_i(E)\tilde{\tau}_i, \quad (2.32)$$

where the operators  $t_{0i}$  and  $g_i$  are defined to be

$$t_{0i} = v_{0i} + v_{0i}g_it_{0i} \quad (2.33)$$

and

$$g_i = [(E - E^i) - h_0 - h_i + i\varepsilon]^{-1}. \quad (2.34)$$

The quantity  $W_i$  represents the coupling of the struck target nucleon to the residual nucleus. At this point, one could take the attitude that a proper consideration of this quantity is not of first order, and it should be put together with the next higher order in the Spectator Expansion. In that case one would obtain the so-called ' $t^{free}$ ' or impulse

approximation to the optical potential, which can be viewed as  $\hat{\tau}_i \approx \tilde{\tau}_i \approx t_{0i}$ . In the case of the impulse approximation, one never needs to solve any integral equation for more than two particles. This has made the impulse approximation very practical in intermediate energy nuclear physics and has over many years led to a large body of work being based upon this approximation [8].

### C. Coupling of the Struck Target Nucleon to the Nucleus

In the explicit treatment of the propagator  $G_i(E)$  it is necessary to consider specific forms of the potential  $W_i$ , which represents the coupling of the struck nucleon to the residual nucleus. In this paper  $W_i$  is treated as one-body operator, such as a shell-model or mean field potential. The attitude is taken here that this potential is already known and is extracted from single particle mean field potentials as calculated in various studies of nuclear structure. In this specific case, Eq. (2.32) can be written as

$$\tilde{\tau}_i = t_{0i} + t_{0i}g_i\mathcal{T}_ig_i\tilde{\tau}_i, \quad (2.35)$$

with  $\mathcal{T}_i$  being given as the solution of a Lippmann-Schwinger type equation with the potential  $W_i$  as the driving term

$$\mathcal{T}_i = W_i + W_ig_i\mathcal{T}_i. \quad (2.36)$$

This is the approach taken in the calculations presented in this paper as well as in earlier work [9–11]. While Eqs. (2.35, 2.36) are completely equivalent to Eq. (2.32), a justification for the substitution of a Hartree-Fock or any other single particle mean field potential taken from a nuclear structure calculation is not strictly within the theoretical prerequisites of the Spectator Expansion, which demands that all of the two-body interactions be consistently represented by  $v_{0i}$ . Standard mean field or shell model calculations use an effective NN interaction for the reason that present microscopic nuclear structure calculations are unable simultaneously to use realistic free NN potentials and predict the experimental results. Hence

it is not physically unreasonable to substitute a mean field potential for  $W_i$ , but this choice is *defacto* outside the strict demands of the Spectator Expansion.

Using the expression given in Eq. (2.27), for  $W_i$ , Eq. (2.32) can be reformulated as

$$\begin{aligned}
\tilde{\tau}_i &= t_{0i} + t_{0i}g_i \sum_{j \neq i} v_{ij} \left[ \frac{1}{g_i^{-1} - \sum_{k \neq i} v_{ik} + i\varepsilon} \right] \tilde{\tau}_i \\
&= t_{0i} + t_{0i}g_i \sum_{j \neq i} v_{ij} \left[ \frac{1}{g_i^{-1} - v_{ij} + i\varepsilon} \right. \\
&\quad \left. + \sum_{j \neq i} v_{ij} \frac{1}{g_i^{-1} - v_{ij} + i\varepsilon} \sum_{k \neq i, j} v_{ik} \frac{1}{g_i^{-1} - \sum_{l \neq i} v_{il} + i\varepsilon} \right] \tilde{\tau}_i \\
&= \bar{\tau}_i + \bar{\tau}_i g_i \sum_{j \neq i} v_{ij} \frac{1}{g_i^{-1} - v_{ij} + i\varepsilon} \sum_{k \neq i, j} v_{ik} \frac{1}{g_i^{-1} - \sum_{l \neq i} v_{il} + i\varepsilon} \tilde{\tau}_i,
\end{aligned} \tag{2.37}$$

where

$$\bar{\tau}_i = t_{0i} + t_{0i}g_i \sum_{j \neq i} t_{ij}g_i \bar{\tau}_i, \tag{2.38}$$

and

$$t_{ij} = v_{ij} + v_{ij}g_it_{ij}. \tag{2.39}$$

Since the last term in Eq. (2.37) always involves at least three different target particles  $(i, j, k)$ , this term is of higher order and is safely neglected at present. Thus the operator  $\tilde{\tau}_i$  can be written as

$$\begin{aligned}
\tilde{\tau}_i &= \bar{\tau}_i + \cdots \\
&= t_{0i} + \sum_{j \neq i} \eta_{ij} + \cdots
\end{aligned} \tag{2.40}$$

where

$$\begin{aligned}
\sum_{j \neq i} \eta_{ij} &\equiv \bar{\tau}_i - t_{0i} \\
\eta_{ij} &= t_{0i}g_it_{ij}g_it_{0i} + t_{0i}g_it_{ij}g_i\eta_{ij},
\end{aligned} \tag{2.41}$$

where  $\eta_{ij}$  neglects the terms involving three target nucleons that arise from Eq. (2.37). This treatment of the interaction of the struck target nucleon with the residual nucleus, though more complicated, is completely consistent with the spirit of the Spectator Expansion.

The term  $\sum_{j \neq i} \eta_{ij}$  involves two active target particles and thus represents a second order Spectator Expansion correction to the first order term considered in this paper. In fact, it could equally well be considered together with the second order term  $\tau_{ij}$  shown in Eq. (2.16). We have found it expedient, however, to define the Spectator Expansion as given in Eq. (2.16). Since this expansion is performed in terms of quantities which in themselves contain many-body propagators, each of the ingredients,  $\tilde{\tau}_i$ ,  $\tilde{\tau}_{ij}$ , etc. may themselves be expanded in a spectator expansion. This amounts to expanding the many-body propagator also according to the number of active participants. Another reason to distinguish the corrections to the propagator and the explicit second order term is that the second order terms in Eq. (2.16), correspond to contributions which arise from the  $Q$  space, whereas the second term in Eq. (2.40) remains in the  $P$  elastic space at the first order level.

#### D. The Second Order Term

Since second order corrections in the propagator should at least in principle be considered simultaneously with the second order corrections in the multiple scattering expansion, the second term in Eq. (2.16) is examined in detail. This term may be written as

$$\sum_{i,j \neq i} \tau_{ij} = \sum_{i>j} (\tilde{U}_{ij} - \tau_i - \tau_j). \quad (2.42)$$

The subtraction of the two-body contribution in Eq. (2.42) plays an important role in that any double counting of the two-body term is removed. This also enables us to see explicitly the three-body nature of the second order term. We start from Eq.(2.22), which can be expressed as

$$\begin{aligned} \tilde{U}_{ij} &= (v_{0i} + v_{0j}) + (v_{0i} + v_{0j})G_0(E)\tilde{U}_{ij} - (v_{0i} + v_{0j})G_0(E)P\tilde{U}_{ij} \\ &= \hat{t}_{0ij} - \hat{t}_{0ij}G_0(E)P\tilde{U}_{ij}, \end{aligned} \quad (2.43)$$

where  $\hat{t}_{0ij}$  is defined as

$$\hat{t}_{0ij} = (v_{0i} + v_{0j}) + (v_{0i} + v_{0j})G_0(E)\hat{t}_{0ij}. \quad (2.44)$$

Thus  $\langle \Phi_A | \tilde{U}_{ij} | \Phi_A \rangle$  is obtained from  $\langle \Phi_A | \hat{t}_{0ij} | \Phi_A \rangle$  through the solution of a straightforward one-body integral equation in a way similar to the manner  $\langle \Phi_A | \tau_i | \Phi_A \rangle$  is obtained from  $\langle \Phi_A | \hat{\tau}_i | \Phi_A \rangle$ . In this case Eq. (2.44) is a full three-body equation.

Once again notice that the propagator  $G_0(E)$  in Eq. (2.44) is a complicated many-body operator. Consistent with the spirit of the Spectator Expansion the propagator can be written as

$$G_0(E) = \left[ (E - h_0 - H^{ij} + i\varepsilon) - h_i - h_j - v_{ij} - \sum_{k \neq i,j} (v_{ik} + v_{jk}) \right]^{-1} \quad (2.45)$$

and a three particle Greens function is defined to be

$$G_{ij}(E) = \left[ (E - E^{ij} - h_0 + i\varepsilon) - h_i - h_j - v_{ij} \right]^{-1}. \quad (2.46)$$

Using the same procedure used in the first order term,  $G_{ij}(E)$  is substituted for  $G_0(E)$  in Eq. (2.44) to obtain

$$\tilde{t}_{0ij} = (v_{0i} + v_{0j}) + (v_{0i} + v_{0j})G_{ij}\tilde{t}_{0ij}, \quad (2.47)$$

where the effective 3-body t-matrix becomes

$$\hat{t}_{0ij} = \tilde{t}_{0ij} + \dots. \quad (2.48)$$

The truncation of the propagator  $G_0(E)$  from Eq. (2.45) to the form given in Eq. (2.46) is once again tantamount to relegating the coupling of the active target nucleons to the next higher order term in the expansion of the propagator.

Actual calculations of the three-body corrections to the first order optical potential as given in Eq. (2.41) and Eq. (2.47) are extraordinarily difficult without further approximations. In this paper we do not attempt to calculate these higher order contributions to the Spectator Expansion. But for the sake of conceptual clarity the propagator corrections in first order, as presented in this work, should be seen in the context of the next higher order of the Spectator Expansion, since both are given through three-body type equations.

### III. RESULTS AND DISCUSSION

#### A. Details of the Calculation

In this paper the study of the elastic scattering of neutrons and protons from spin zero target nuclei at energies that range from 65 and 400 MeV (incident projectile energy) is strictly first order in the Spectator Expansion. Here the correction to the propagator  $G_0(E)$  due to the coupling of the initially struck target nucleon to the residual target is considered to be first order. As outlined in subsection C of the previous section this calculation includes the modification of the free propagator due to the ‘nuclear medium’. The operator  $\mathcal{T}_i$ , representing the scattering of the struck target particle  $i$  from the residual nucleus, is calculated through the use of a one-body potential  $W_i$ . Nonlocal, spin-dependent potentials derived from realistic nuclear mean field models are used to represent the potential  $W_i$  given in Eq. (2.36). Two different mean field potentials are used in these calculations in order to isolate any model dependence which may exist. One is the nonrelativistic, non-local mean field potential taken from a Hartree-Fock-Bogolyubov microscopic nuclear structure calculation, which utilizes the density-dependent finite-ranged *Gogny D1S* nucleon-nucleon interaction [12,13]. This model has been shown to provide accurate descriptions of a variety of nuclear structure effects. Calculations using this potential as  $W_i$  will be referred to as HFB. The second choice involves a nonrelativistic, local reduction of the mean field potential resulting from a Dirac-Hartree calculation based upon the  $\sigma - \omega$  model [14]. The calculations with this potential will be referred to as DH. Comparisons of calculations with these two models may serve to indicate the sensitivity of the elastic scattering predictions to the model of the nuclear mean field potential. The results suggest that there is a slight sensitivity to the choice of the mean field potential, however this ‘uncertainty’ is smaller than the overall size of the medium correction. One might therefore expect that any reasonable model of this kind, which describes nuclear structure could give qualitatively similar results. A step by step description of the implementation of the nuclear mean field potential, consistent with

the framework of the Spectator Expansion is given in Ref. [9].

The treatment of the propagator modification through a nuclear mean field potential taken from structure calculations, although a valid approach, may not be completely satisfactory. In keeping full consistency with the theory of multiple scattering, it may be better to treat the operator  $\mathcal{T}_i$  as

$$\mathcal{T}_i = \sum_{j \neq i} t_{ij} + \dots \quad (3.1)$$

as outlined in subsection C of the previous section of Eqs. (2.40) and (2.41), where  $t_{ij}$  is defined in Eq. (2.38)]. Calculations based on this approach are much more difficult than any performed so far, and though not intrinsically intractable, have been postponed. The structure of Eqs. (2.40) and (2.41) is very similar to the calculation of the second order in the Spectator Expansion as outlined in subsection D of the previous section, and both should be treated in the same order and in a similar manner. Further, note that an approximate treatment of the three-body kinematics involving the scattering of the struck target nucleon from the residual nucleus is used and is discussed in length in Ref. [9].

The nucleon-nucleon (NN) t-matrix is another crucial ingredient in these calculations. The quality and extensiveness of the nucleon-nucleus observables we attempt to predict require trustworthy representations of the NN interaction. For convenience the calculations presented here use the free NN interaction based upon the full Bonn potential [15], giving  $t_{oi} = t_{oi}^{free}$ . This interaction includes the effects of relativistic kinematics, retarded meson propagators as given by time-ordered perturbation theory, and crossed and iterative meson exchanges with NN,  $N\Delta$ , and  $\Delta\Delta$  intermediate states. A comparison of nucleon-nucleus observables based on different models for the NN interaction is deferred to a later time. It should be clearly stated that even if the underlying models for the NN interaction accurately describe the ‘on-shell’ NN data, there may still exist ‘off-shell’ differences between the various models, which could affect the predictions of the elastic nucleon-nucleus observables.

The first order folded effective NN t-matrix is then constructed with the operator,

$\tilde{\tau}_i$ , from Eq. (2.35):

$$\langle \tilde{\tau}_{eff} \rangle = \langle \vec{k}'_0 \Psi_A | \sum_i \tilde{\tau}_i | \vec{k}_0 \Psi_A \rangle . \quad (3.2)$$

These calculations are performed in momentum space and include spin degrees of freedom. The first order optical potential is then evaluated by solving Eq. (2.23) in the folded form. In the present calculations, which are performed in momentum space,  $\langle \tilde{\tau}_{eff} \rangle$  enters in the ‘optimum factorized’ or ‘off-shell  $\tau\rho$ ’ form [16,17] as

$$\langle \tilde{\tau}_{eff} \rangle \approx \tilde{\tau}(q, \mathcal{K}; E) \rho(q) , \quad (3.3)$$

where  $\vec{q} = \vec{k}'_0 - \vec{k}_0$  and  $\vec{\mathcal{K}} = \frac{1}{2} (\vec{k}'_0 + \vec{k}_0)$ ;  $\vec{k}'_0$  and  $\vec{k}_0$  are the final and initial momenta of the projectile. This corresponds to a steepest descent evaluation of the ‘full-folding’ integral, in which the non-local operator  $\tilde{\tau}$  is convoluted with the density  $\rho(q)$  as indicated schematically in Eq. (3.2). For harmonic oscillator model densities it has been shown that the optimum factorized form represents the nonlocal character of  $U_{opt}$  qualitatively in the intermediate energy regime [18,19]. Complete ‘full-folding’ calculations with more realistic nuclear densities are in progress. It is to be understood that we perform all spin summations in obtaining  $U_{opt}$ . This reduces the required NN t-matrix elements to a spin-independent component (corresponding to the Wolfenstein amplitude  $A$ ) and a spin-orbit component (corresponding to the Wolfenstein amplitude  $C$ ). All scattering calculations presented here contain an additional factor in the optical potential to account for the transformation of the NN t-matrix from the two-nucleon c.m. frame to the nucleon-nucleus c.m. frame [17].

Another uncertainty in the present calculations lies in the lack of completely reliable target wave functions of the accuracy required. The best guide for the distribution of matter in nuclei is the information extracted from electron scattering [20]. This information gives a reasonably good picture of the average single particle proton density especially about the surface, and it is used in the calculations presented in this paper to represent the proton densities. The neutron densities used are those taken from the Hartree-Fock-Bogolyubov calculation described above [12]. In principle, it would appear more consistent to employ the

proton densities obtained from the same calculation. However, there are small differences between the calculated proton densities and the measured ones. These small differences are, however, large enough to influence slightly the predictions of the nucleon-nucleus observables. Therefore, the measured proton distributions were thought to be more reliable and are used throughout the present calculations. This does leave a question about the reliability of the calculated neutron distributions which were used in the present calculations. A study on the sensitivity of the proton-nucleus observables to slight variations in the neutron distributions was presented in Ref. [21].

For the proton-nucleus scattering calculations the Coulomb interaction between the projectile and the target is included using the exact formalism described in Ref. [22]. Although the multiple scattering calculations are performed fully in momentum space, so as to be able to include easily nonlocal and off-shell effects, the point Coulomb contributions are described by using Coulomb scattering wave functions in coordinate space. There are no cut-off parameters necessary in this technique.

## B. Total Cross Section for Neutron Scattering

In nuclear structure calculations the binding energy of the system in its ground state together with energies of certain low lying excited states are the experimental information which must be closely reproduced to establish the reliability of the model wave functions and the various physical matrix elements implied thereby. In the present calculations of elastic nucleon-nucleus scattering the neutron total cross section, as a function of scattering energy, should serve as a similar figure of merit. In the early 1990's extensive high precision measurements of neutron total cross sections became available for a variety of target nuclei [23,24] and can now be used to discriminate between scattering calculations in the above indicated fashion.

In Fig. 1 total neutron cross section data for  $^{12}\text{C}$ ,  $^{16}\text{O}$ ,  $^{28}\text{Si}$ ,  $^{40}\text{Ca}$ ,  $^{90}\text{Zr}$  and  $^{208}\text{Pb}$  are shown along with various calculations of  $\sigma_{tot}(E)$  at a number of energies. Because the

data are so extensive, the ‘usual’ procedure has been reversed and the data are represented by dotted curves. The ‘jitter’ in these curves may be taken as indicative of the experimental uncertainty. The statistical error bars themselves are of the order of 1% and could not be distinguished in the figures. The discrete points correspond to the calculated results. The solid diamonds represent the calculations as described in Section A and include the modification of the free propagator through the Hartree-Fock-Bogolyubov mean field [12], except for  $^{208}\text{Pb}$  where  $W_i$  is taken from the DH case. In each case the predictions are in accord with the data from  $\gtrsim 65$  MeV for the light nuclei and  $\gtrsim 100$  MeV for the heavier nuclei. That is, the theoretical predictions do extremely well in predicting the energy dependence of the total neutron cross section beyond the point where the data exhibit a pronounced structure.

Since a detailed discussion on the description of neutron total cross sections for  $^{16}\text{O}$  and  $^{40}\text{Ca}$  was recently published [10] comments on this subject will be somewhat restricted. As an indication as to how much has been gained by eliminating necessary earlier approximations to the full first order theory, points, represented as crosses, are shown at 100 and 200 MeV for  $^{16}\text{O}$ ,  $^{40}\text{Ca}$ ,  $^{90}\text{Zr}$  and  $^{208}\text{Pb}$  which were calculated using the so-called ‘local free  $\tau\rho$ ’ approximation. This consists of multiplying the on-shell NN scattering amplitude  $t(q)$  with the one nucleon density  $\rho(q)$  for the target nucleus. For many years this simple approximation was taken to represent the first order theory (of course, it was not possible to perform more difficult calculations at that time). The total cross sections calculated this way are invariably above the full calculation represented by the solid diamonds. These ‘local free  $\tau\rho$ ’ results are also significantly larger than the experimental values, in some cases, especially for the heavier elements, this discrepancy can be as large as 25 – 30%. This gross failure of the local approximation casts serious doubt upon some of its early successes, and certainly creates serious reservations about the many attempts to account for the failures of the local approximation by the introduction of new effects, which are not cleanly consistent with a many-body scattering theory.

Of greater current interest is the difference between the points represented as stars

and the solid diamonds. The stars are calculations performed with the free propagator  $G_0(E)$  of Eq. (2.26), where the target Hamiltonian  $H_A$  is approximated by a c-number. Therefore these points contain the complete off-shell structure of the NN t-matrix, but neglect the coupling of the struck target nucleon to the residual nucleus. The difference between the stars and the solid diamonds represent the size of this effect, i.e. the coupling of the struck target nucleon to the residual nucleus. As Fig. 1 shows, and as expected, the absolute size of the effect grows as the nuclei become heavier. In addition it is most prevalent in the regime between 100 and 200 MeV projectile energy and becomes almost negligible at higher energies. For all nuclei under consideration at 300 and 400 MeV the propagator modification has no discernible effect. It is most satisfying to observe that whenever this correction is significant, it moves the calculated results closer to the measurements.

### C. Proton Elastic Scattering Observables

Obviously there are no comparable total cross section data for proton scattering. On the other hand, there is relatively little experimental information on elastic angular distributions and no spin-observables for neutron scattering from nuclei. Thus for a more detailed look at nucleon-nucleus elastic scattering, the scattering of protons from nuclei is examined. For the proton case the Coulomb interaction between the projectile and the target is included using the exact method developed in Refs. [22]. In a recent paper [11] elastic proton and neutron scattering observables at 65 MeV projectile energy for  $^{12}\text{C}$ ,  $^{16}\text{O}$ ,  $^{28}\text{Si}$ ,  $^{40}\text{Ca}$ ,  $^{90}\text{Zr}$  and  $^{208}\text{Pb}$  were shown. These calculations were performed at an energy which was considered by many to be below the regime of applicability of the first order Spectator Expansion. However there is a wealth of experimental data at this energy for the above mentioned nuclei. This data includes the differential cross section  $\frac{d\sigma}{d\Omega}$ , the analyzing power  $A_y$  and the spin rotation function  $Q$  (with the exception that for  $^{28}\text{Si}$  and  $^{56}\text{Fe}$  there are no measurements of  $Q$ ). At this low energy fairly good agreement between the predictions and the measurements was observed. It was very clear that the inclusion of the coupling

of the struck target nucleon to the residual nucleus considerably improved the description of the data. This was especially true for the description of the spin rotation parameter  $Q$ , in which case the improvement was dramatic. In this paper further calculations at other energies in the regime between 80 and 300 MeV are presented. Elastic proton scattering observables are calculated for a variety of light as well as heavy spin-zero targets at a variety of energies. Here predictions are presented only for those targets and energies where spin observable data exist. Unfortunately in the regime below 200 MeV, there is no other energy like 65 MeV where the proton spin observables have been measured for many nuclei in a similarly systematic manner.

The calculations chosen here are limited to energies below pion-production threshold. The reason is twofold. First, the NN  $t$ -matrix, which represents one of the critical inputs to the calculations is not as well established at higher energies. Second, the correction to the free propagator due to the presence of the nuclear medium, which is the new ingredient in these calculations decreases in importance as the energy increases. This is shown for the total cross section in Fig. 1. In Figs. 2-14 the angular distribution, the analyzing power and the spin rotation function for elastic proton scattering are shown for  $^{12}\text{C}$  at 200 MeV;  $^{16}\text{O}$  at 100, 200, and 318 MeV,  $^{28}\text{Si}$  at 80, 135 and 200 MeV,  $^{40}\text{Ca}$  at 80 MeV,  $^{90}\text{Zr}$  at 65, 80 and 160 MeV, and  $^{208}\text{Pb}$  at 80 and 200 MeV, respectively.

To show the dependence on the choice of the mean field potential  $W_i$  (Eqs. (2.30) and (2.32)) calculations with two different mean field potentials representing the operator  $W_i$  are displayed. The solid line corresponds to the results based upon the HFB potential [12], whereas the dashed curve is based upon the DH potential [14]. For the calculations of proton scattering from  $^{208}\text{Pb}$  the DH mean field potential only is used (solid line), since the choice and size of the basis function representing  $W_i$  was not adequate for the HFB mean field potential in this case. Calculations, where no medium contributions are included, correspond to the free ‘off-shell  $t\rho$ ’ approximation and are given by the dash-dotted line.

The figures show that both calculations which incorporate the coupling of the struck nucleon to the residual nucleus provide a good representation of the data except at

very large scattering angles. That this description, while very good, is not perfect is easily understandable since various corrections to the many body theory still remain unexplored. The calculations are limited to lowest order in the spectator expansion, and are carried out in the optimum factorized form, which takes only the non-local structure of the NN t-matrix into account. Finally, the full three-body structure involved in the coupling of the struck nucleon to the residual nucleus has not yet been considered. In addition, for large angles the Pauli exchange of the Coulomb term could play a role. Those effects are not included in the present calculations.

For the lighter target nuclei in Figs. 2-8 the correction to the propagator causes the diffraction minima in the predictions to move slightly to higher angles and be closer to the data. The improvement of the theoretical predictions is more apparent in the spin observables, especially in Fig. 6. At lower energies (Figs. 3, 6, and 9) the propagator modifications causes a characteristic shift of the spin rotation function  $Q$ . Unfortunately there are no measurements of  $Q$  at the energies presented here. In an earlier work [11], presenting only calculations at 65 MeV projectile energy, the propagator modification brought the calculations in excellent agreement with the measured values for  $Q$ . So we expect that measurements of  $Q$  around 100 MeV would also be close to our calculations. At projectile kinetic energies of 200 MeV or above the full calculations provide very good results with respect to the data. The modification of the propagator effect only  $A_y$  in a very moderate fashion.

For the heavier nuclei in Figs. 10-14 one would expect the effects of the medium modifying the propagator to be more pronounced, which is indeed the case. The shift of the diffraction minima to larger angles is clearly visible for the heavy nuclei  $^{90}\text{Zr}$  and  $^{208}\text{Pb}$ , especially at lower energies (Fig. 10, 11, and 12). For  $^{90}\text{Zr}$  at 65 MeV (Fig. 10) the propagator modification has a significant effect on the observables. The minima in the diffraction pattern of the differential cross section coincide with the measured ones, indicating a correct prediction of the size of the nucleus. Furthermore, the overall size of  $d\sigma/d\Omega$  is predicted correctly over about five orders of magnitude. The effect on the spin observables is equally

dramatic and causes the predictions of  $A_y$  and  $Q$  to agree remarkably well with the data. We included Fig. 10, though already being published in Ref. [11], since at lower energies the only measurements of  $Q$  exist at 65 MeV. Again, for  $^{90}\text{Zr}$  at 80 MeV (Fig. 11) the propagator modification has a significant effect on the differential cross section and the spin observables and causes the predictions of  $A_y$  to agree very well with the data. A similar tendency can be seen for  $^{208}\text{Pb}$  at the same energy (Fig. 13). At 160 MeV the medium effects are not as pronounced for  $^{90}\text{Zr}$  except at larger angles where the full calculation provides better agreement with the data (Fig. 12). For  $^{208}\text{Pb}$  at 200 MeV in Fig. 14 in the spin rotation there are differences caused by the modification of the propagator, but the effects on the predictions of the data are unclear.

In order to indicate the progress which has been made in the calculation of proton-nucleus elastic scattering, results for selected cases obtained with the local, ‘on-shell  $t\rho$ ’ approximation are shown, where the off-shell contributions of both, the NN t-matrix as well as the density matrix are neglected. Those ‘local’ calculations are represented by the dotted lines in Figs. 3, 4, and 14 for  $^{16}\text{O}$  at 100 and 200 MeV and for  $^{208}\text{Pb}$  at 200 MeV, respectively. As was already the case for the description of neutron total cross sections, the local calculations show moderate deficiencies for a light nucleus like  $^{16}\text{O}$ , manifested in an overprediction of the differential cross section, a lack of structure in the spin observable  $A_y$ , and differences in the spin rotation function  $Q$ . For a heavy nucleus like  $^{208}\text{Pb}$  the local calculation looks disastrous, leading already to a severe overprediction of the size of the nucleus as seen in the diffraction pattern of the differential cross section. This lack of agreement led in the past to the study of corrections to the local approximation specifically in heavy nuclei [8]. It is a very satisfactory result for us to find that the first order calculation in the Spectator Expansion together with a consistent treatment of the propagator modification leads to a good description of the elastic proton-nucleus observables for light as well as heavy nuclei in the energy regime especially between  $\sim 65$  and 400 MeV projectile energy.

## IV. CONCLUSION

The Spectator Expansion of Multiple Scattering Theory is described in detail. The optical potential is expanded into a series predicated upon the idea that the dominant effect is the two-body interaction between the projectile and one of the nucleons in the target. The number of target nucleons interacting directly with the projectile determines the ordering of the scattering series. Complexities due to the free many-body propagator for the projectile – target system also play a significant role and are treated within a consistent theoretical framework within the Spectator Expansion. The first order theory and the treatment of the many-body propagator due to effects from the residual nucleus are presented, along with a formal description of the second-order contribution.

Predictions from rigorous calculations of elastic nucleon-nucleus scattering at projectile kinetic energies in the range  $\sim 65$  to 400 MeV provide excellent agreement with the experimental data. In this case the basic inputs to the calculation are the free fully off-shell NN interactions and realistic nuclear densities. Modifications to the propagator were calculated using static potentials taken from microscopic mean field structure calculations. It is found that as the calculations include more complex degrees of freedom within a well-defined theoretical framework, the predictions invariably provide an improved description of the data. The first order Spectator Expansion provides an excellent *a priori* description of the extensive data for nucleon-nucleus scattering data from  $\sim 65$  to 400 MeV for modest momentum transfers. These results are in fact good enough to encourage speculation that further work may soon yield new information about neutron distributions and nuclear correlations in nuclei.

## ACKNOWLEDGMENTS

The computational support of the the Ohio Supercomputer Center under Grants No. PHS206 and PDS150 is gratefully acknowledged. This work was performed in part under the auspices of the U. S. Department of Energy under contracts No. DE-FG02-93ER40756 with Ohio University, DE-AC05-84OR21400 with Martin Marietta Energy Systems, Inc., and DE-FG05-87ER40376 with Vanderbilt University. This research has also been supported in part by the U.S. Department of Energy, Office of Scientific Computing under the High Performance Computing and Communications Program (HPCC) as a Grand Challenge project titled ‘the Quantum Structure of Matter’.

## REFERENCES

- [1] K.M. Watson, Phys. Rev. **89**, 575 (1953); N.C. Francis and K. M. Watson, *ibid.* **92**, 291 (1953).
- [2] A. Kerman, M. McManus, and R. M. Thaler, Ann. Phys. **8**, 551 (1959).
- [3] D.J. Ernst, J.T. Londergan, G.A. Miller, and R.M. Thaler, Phys. Rev. **C16**, 537 (1977).
- [4] E. R. Siciliano and R. M. Thaler, Phys. Rev. **C16**, 1322 (1977).
- [5] P.C. Tandy and R.M. Thaler, Phys. Rev. **C22**, 2321 (1980).
- [6] R. Crespo, R.C. Johnson, and J.A. Tostevin, Phys. Rev. **C48**, 351 (1993), *ibid.* **C46**, 279 (1992), *ibid.* **C44**, R1735 (1991) and further references therein.
- [7] See for example a review by B.H. Brandow, Rev. Mod. Phys. **39**, 771 (1967).
- [8] see for example L. Ray, G.W. Hoffmann, and W.R. Coker, Phys. Rep. **212**, 223 (1992) and references therein.
- [9] C.R. Chinn, Ch. Elster, and R.M. Thaler, Phys. Rev. **C48**, 2956 (1993).
- [10] C.R. Chinn, Ch. Elster, R.M. Thaler, and S.P. Weppner, Phys. Rev. **C51**, 1033 (1995).
- [11] C.R. Chinn, Ch. Elster, R.M. Thaler, and S.P. Weppner, to appear in Phys. Rev. C.
- [12] See for example J.F. Berger, M. Girod, and D. Gogny, Nucl. Phys. **A502**, 85c (1989); J.P. Delaroche, M. Girod, J. Libert and I. Deloncle, Phys. Lett. **B232**, 145 (1989).
- [13] J.F. Berger, M. Girod, and D. Gogny, Comput. Phys. Commun. **63**, 365 (1991).
- [14] C.J. Horowitz and B.D. Serot, Nucl. Phys **A368**, 503 (1981).
- [15] R. Machleidt, K. Holinde, and Ch. Elster, Phys. Rep. **149**, (1987).
- [16] D. J. Ernst and G. A. Miller, Phys. Rev. C **21**, 1472 (1980); D. L. Weiss and D. J. Ernst, Phys. Rev. C **26**, 605 (1982); D. J. Ernst, G. A. Miller and D. L. Weiss, Phys. Rev. C

- 27, 2733 (1983).
- [17] A. Picklesimer, P. C. Tandy, R. M. Thaler, and D. H. Wolfe, Phys. Rev. **C 30**, 1861 (1984).
  - [18] T. Cheon, Ch. Elster, E. F. Redish, and P. C. Tandy, Phys. Rev. **C41** (1990), 841.
  - [19] R. Crespo, R. C. Johnson, and J. A. Tostevin, Phys. Rev. **C41** (1990), 2257.
  - [20] I. Sick, J. B. Bellicard, J. M. Cavedon, B. Frois, M. Huet, P. Leconte, P. X. Ho, and S. Platchkov, Phys. Lett. **88B**, 245 (1979); B. Frois, J.B. Bellicard, J.M. Cavedon, M. Huet, P. Leconte, P. .Ludeau, A. Nakada, and P.X. Ho, Phys. Rev. Lett. **38**, 152 (1977).
  - [21] C.R. Chinn, Ch. Elster, and R.M. Thaler, Phys. Rev. **C47**, 2242 (1993).
  - [22] C.R. Chinn, Ch. Elster, and R.M. Thaler, Phys. Rev. **C44**, 1569 (1991).
  - [23] R. W. Finlay, W. P. Abfalterer, G. Fink, E. Montei, T Adami, P. W. Lisowski, G. L. Morgan and R. C. Haight, Phys. Rev. **C 47**, 237 (1993).
  - [24] R.W. Finlay, G. Fink, W. Abfalterer, P. Lisowski, G.L. Morgan, and R.C. Haight, in *Proceedings of the Internat. Conference on Nuclear Data for Science and Technology*, edited by S.M. Qaim (Springer-Verlag, Berlin, 1992), p. 702.
  - [25] H.O. Mayer, P. Schwandt, G.L. Mooke, P.P. Singh, Phys. Rev. **C23**, 616 (1981); H.O. Mayer, P. Schwandt, W.W. Jacobs, J.R. Hall, Phys. Rev. **C27**, 459 (1983).
  - [26] H. Seifert, Ph.D thesis, Univ. Maryland (1990).
  - [27] E.J. Stephenson, in ‘Antinucleon- & Nucleon-Nucleus Interactions’ Telluride, Co. 1985, pp 299, ed. by G. Walker et al. (Plenum Press, NY, 1985).
  - [28] J.J. Kelly et al., Phys. Rev. **C43**, 1272 (1991); E. Bleszynski et al., Phys. Rev. **C37**, 1527 (1988).

- [29] C. Olmer, A.D. Bacher, G.T. Emery, W.P. Jones, D.W. Miller, H. Nann, P. Schwandt, S. Yen, T.E. Drake and R.J. Sobie, Phys. Rev. **C29**, 361 (1984).
- [30] P. Schwandt, H.O. Mayer, W.W. Jacobs, A.D. Baches, S.E. Vigdor, M.D. Kartchuck, Phys. Rev. **C26**, 55 (1982).
- [31] J. Liu, A.D. Bacher, S.M. Bowyer, J. Lisantti, C. Olmer, E.J. Stephenson, S.P. Wells, and S.W. Wissink, Annual IUCF Sci. and Tech. Report - 1991, p. 17.
- [32] H. Sakaguchi, M. Nakamura, K. Hatanaka, A. Goto, T. Noro, F. Ohtani, H. Sakamoto, H. Ogawa, and S. Kobayashi, Phys. Rev. **C 26**, 944 (1982).
- [33] A. Nadasen, P. Schwandt, P.P. Singh, W.W. Jacobs, A.D. Bocher, P.T. Debevec, M.D. Katchuck, J.T. Meek, Phys. Rev. **C23**, 1023 (1981).
- [34] D.A. Hutcheon et al. in ‘Polarizion Phenomena in Nuclear Physics - 1980’, Proceedings of the Fifth International Symposium on Polarization Phenomena in Nuclear Physics, AIP Conf. Proc. No. 69, edited by G.G. Ohlson, R.E. Brown, N. Jarmie, W.W. McNaughton, and G.M. Hale (AIP, NY, 1981), p. 454. The data for  $Q$  are from Na Gi, Masters Thesis, Simon Frazer University, British Columbia, 1987.

## FIGURES

FIG. 1. The neutron-nucleus total cross-sections for scattering from  $^{12}\text{C}$ ,  $^{16}\text{O}$ ,  $^{28}\text{Si}$ ,  $^{40}\text{Ca}$ ,  $^{90}\text{Zr}$ , and  $^{208}\text{Pb}$  are shown as a function of the incident neutron kinetic energy. The dotted line represents the data taken from Ref. [23,24]. The solid diamonds correspond to the calculations including the propagator modification due to the HFB mean field [12] (in case of  $^{208}\text{Pb}$  of the DH mean field [14]). The star symbols indicate the ‘free’ calculations using the full Bonn free NN t-matrix [15] only. The cross symbols represent a local ‘on-shell  $t\rho$ ’ calculation, which uses only the on-shell values of the same t-matrix.

FIG. 2. The angular distribution of the differential cross-section ( $\frac{d\sigma}{d\Omega}$ ), analyzing power ( $A_y$ ) and spin rotation function ( $Q$ ) are shown for elastic proton scattering from  $^{12}\text{C}$  at 200 MeV laboratory energy. All calculations are performed with a first-order optical potential obtained from the full Bonn interaction [15] in the optimum factorized form. The solid curve includes the modification of the propagator due to the HFB mean field [12], the dashed curve the one due to the DH mean field [14]. The free impulse approximation is given by the dash-dotted curve. The data are taken from Ref. [25].

FIG. 3. Same as Fig. 2, except for  $^{16}\text{O}$  at 100 MeV proton kinetic energy. The dotted line represents a local ‘on-shell  $t\rho$ ’ calculation which uses only the on-shell values of the same t-matrix. The data are from Ref. [26].

FIG. 4. Same as Fig. 3, except the projectile kinetic energy is 200 MeV. The dotted line represents a local ‘on-shell  $t\rho$ ’ calculation which uses only the on-shell values of the same t-matrix. The data are from Ref. [27].

FIG. 5. Same as Fig. 3, except the projectile kinetic energy is 318 MeV, and the data are from Ref. [28].

FIG. 6. Same as Fig. 2, except for  $^{28}\text{Si}$  at 80 MeV proton kinetic energy. The data are from Ref. [29].

FIG. 7. Same as Fig. 6, except the projectile kinetic energy is 135 MeV, and the data are from Ref. [29,30].

FIG. 8. Same as Fig. 6, except the projectile kinetic energy is 200 MeV, and the data are from Ref. [31].

FIG. 9. Same as Fig. 2, except for  $^{40}\text{Ca}$  at 80 MeV proton kinetic energy. The data are from Ref. [33].

FIG. 10. Same as Fig. 2, except for  $^{90}\text{Zr}$  at 65 MeV proton kinetic energy. The data are from Ref. [32].

FIG. 11. Same as Fig. 10, except for  $^{90}\text{Zr}$  at 80 MeV proton kinetic energy. The data are from Ref. [30].

FIG. 12. Same as Fig. 10, except except the projectile kinetic energy is 160 MeV. The data are from Ref. [30].

FIG. 13. Same as Fig. 2, except for  $^{208}\text{Pb}$  at 80 MeV proton kinetic energy. The data are from Ref. [33].

FIG. 14. Same as Fig. 13, except except the projectile kinetic energy is 200 MeV. The dotted line represents a local ‘on-shell  $t\rho$ ’ calculation which uses only the on-shell values of the same t-matrix. The data are from Ref. [34].

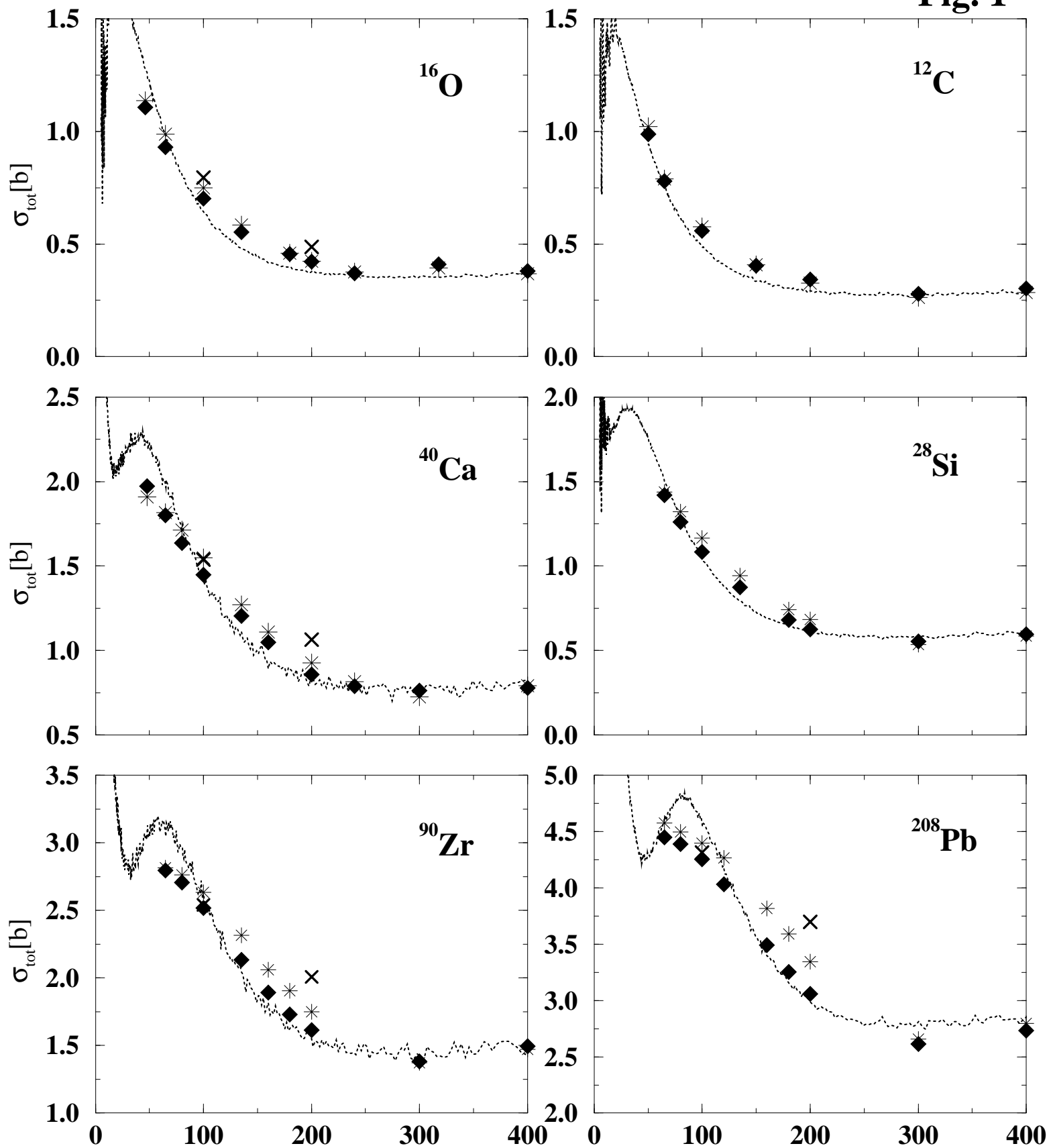
**Fig. 1**

Fig. 2

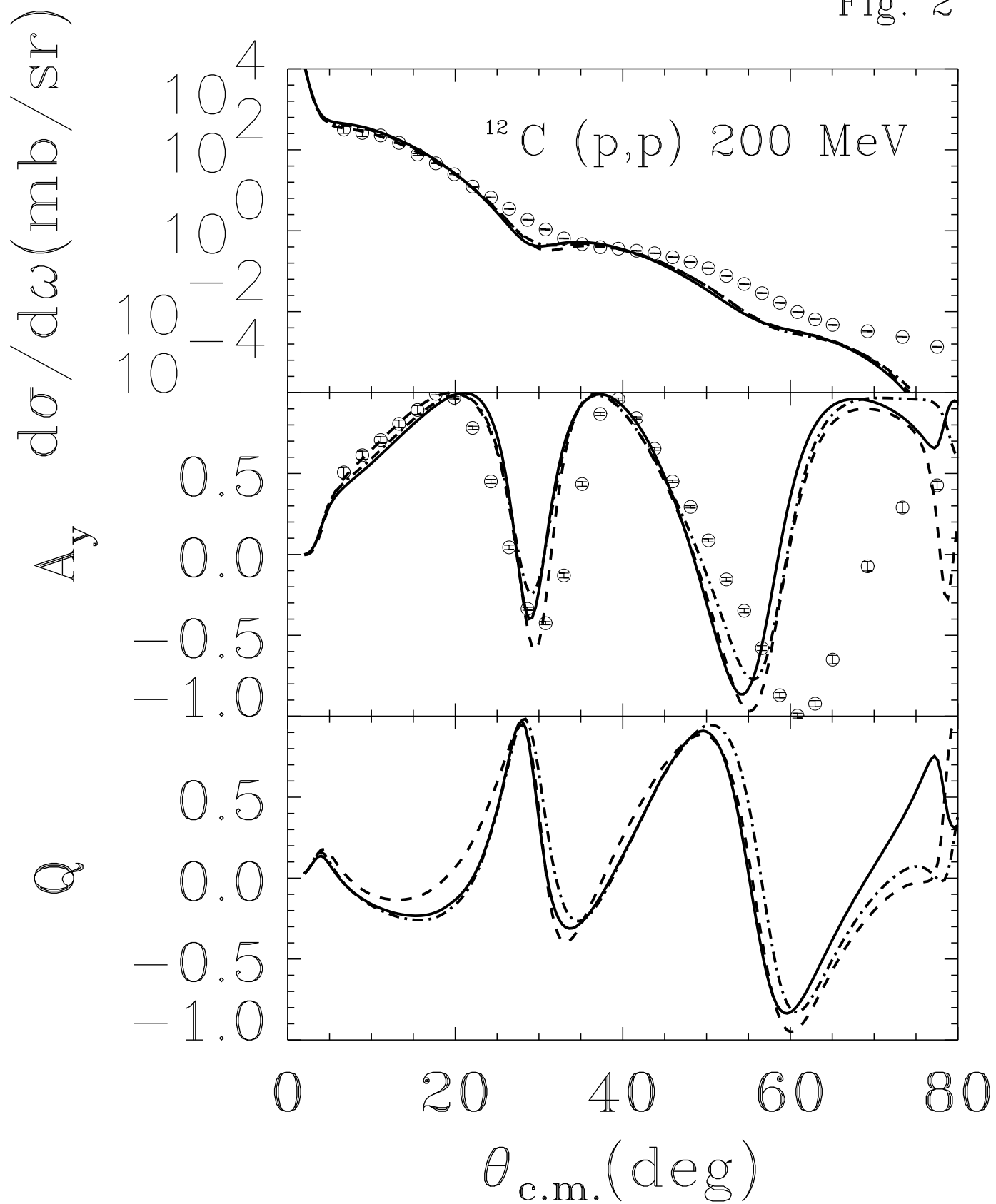


Fig. 3

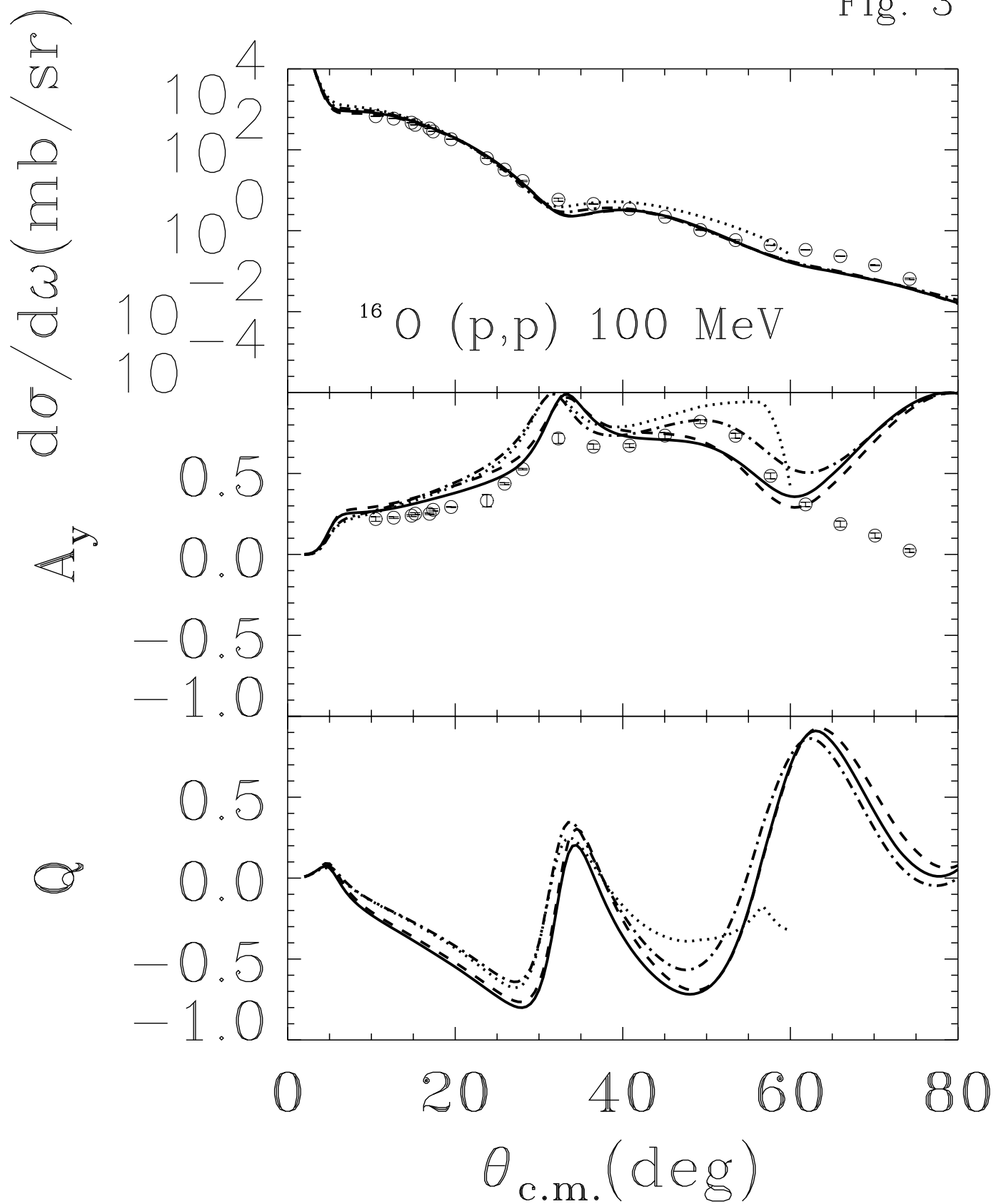


Fig. 4

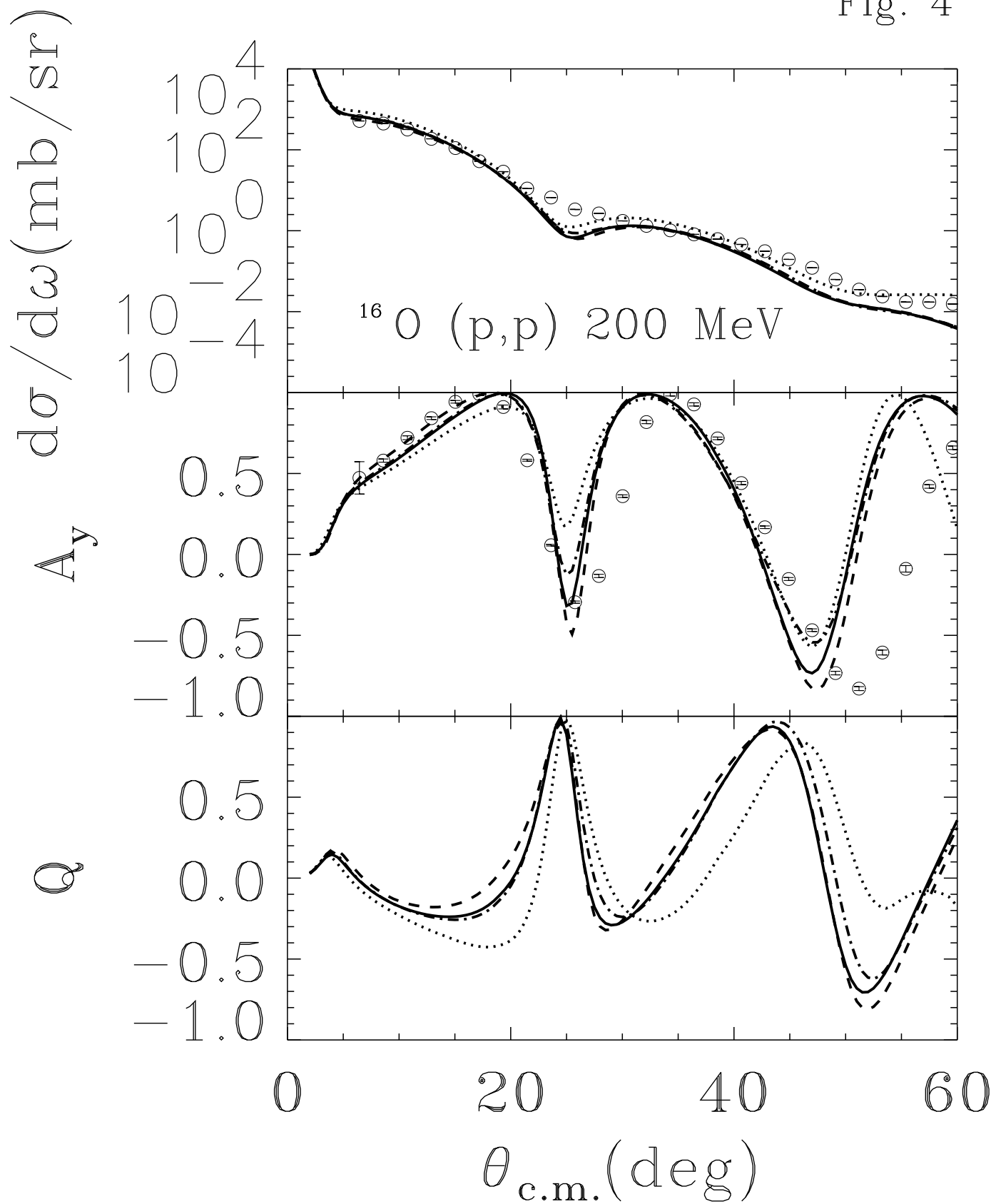


Fig. 5

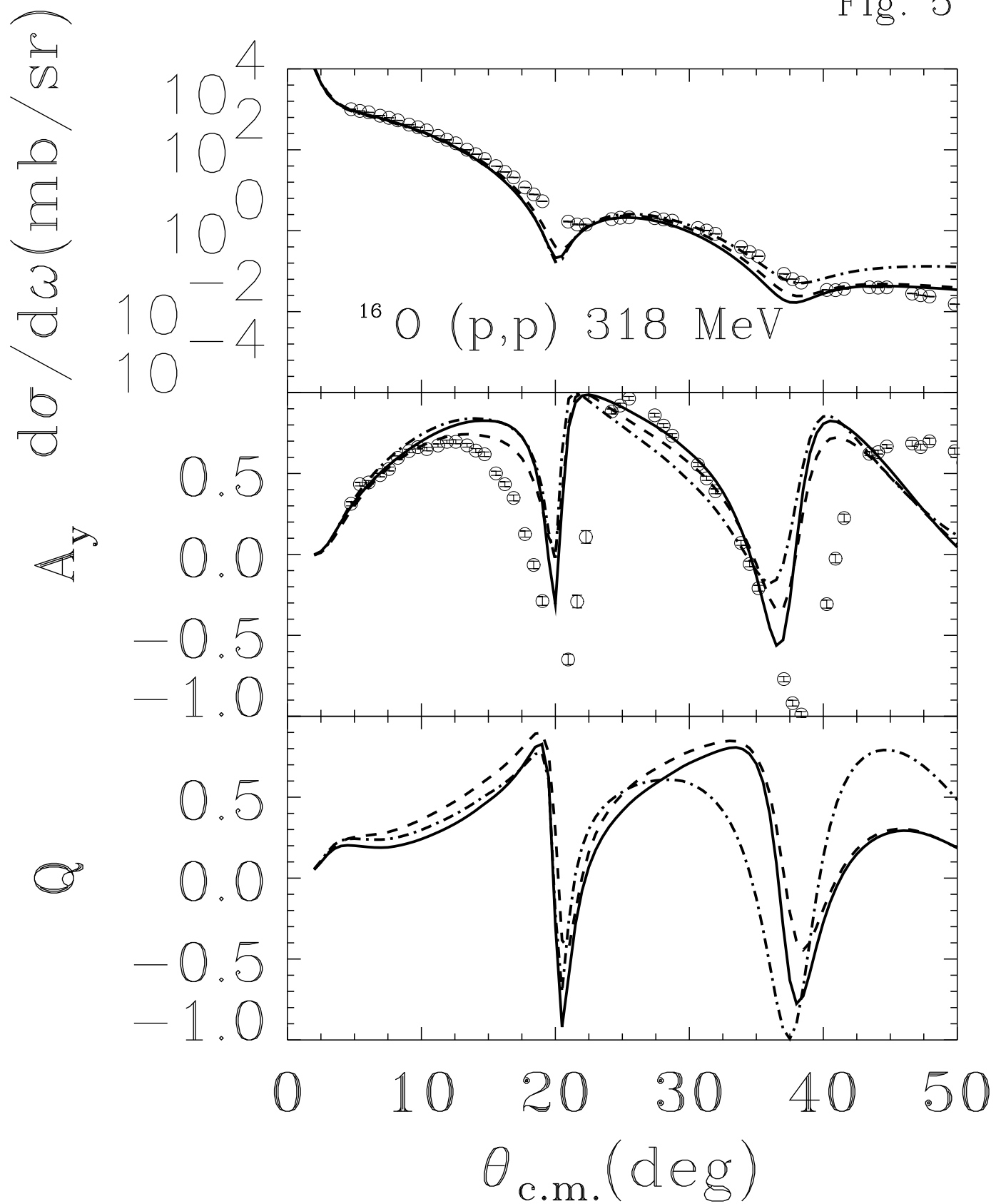


Fig. 6

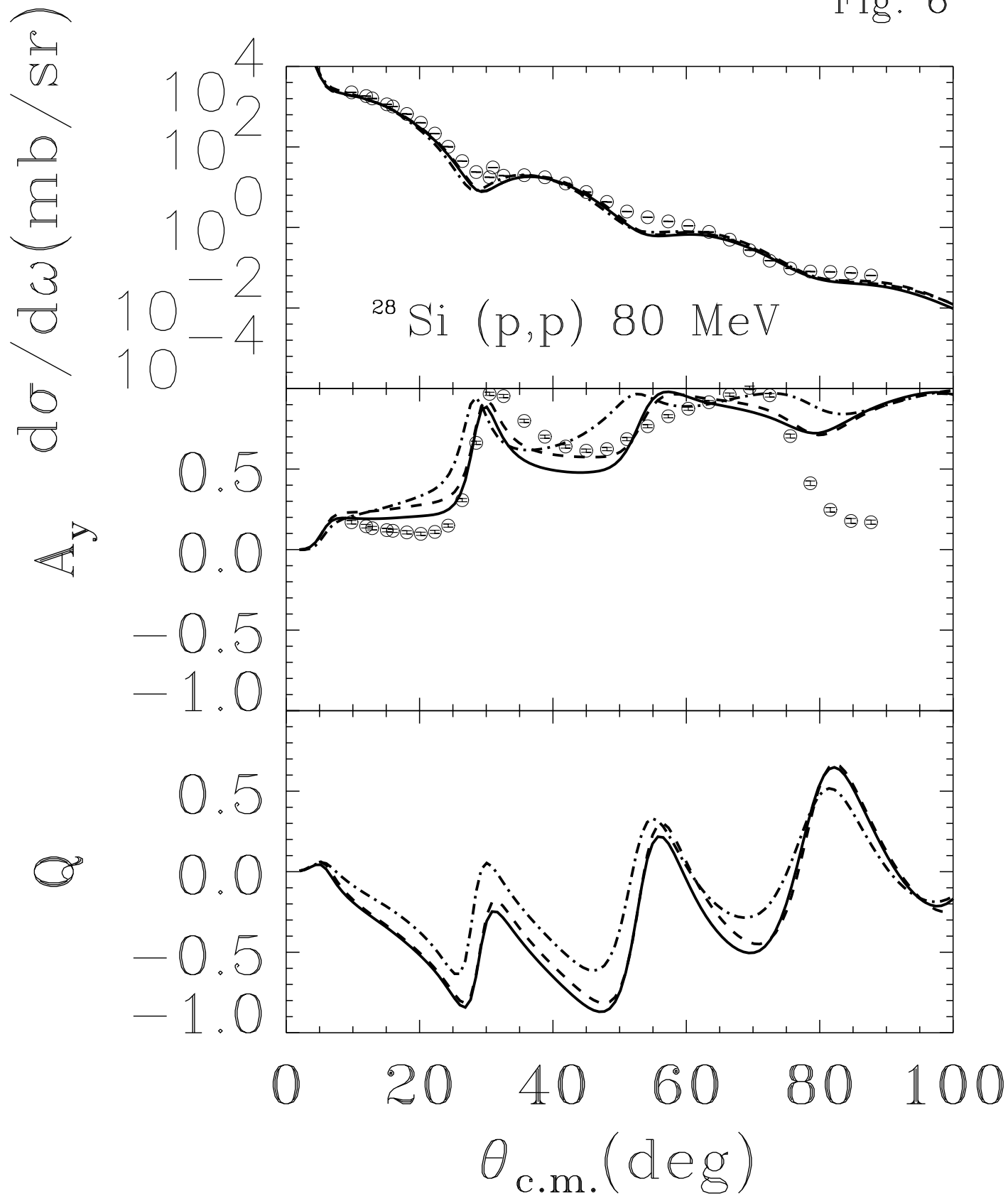


Fig. 7

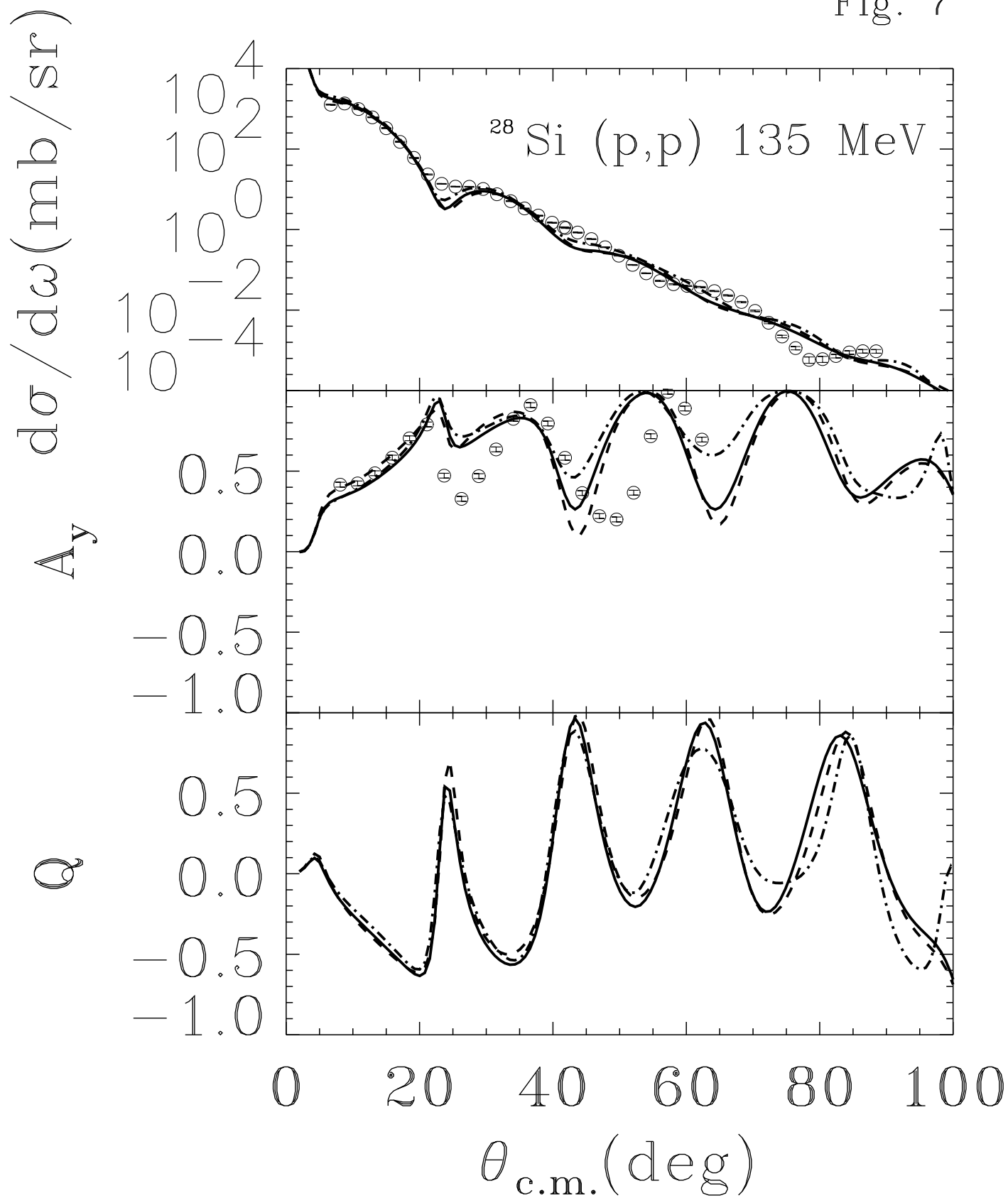


Fig. 8

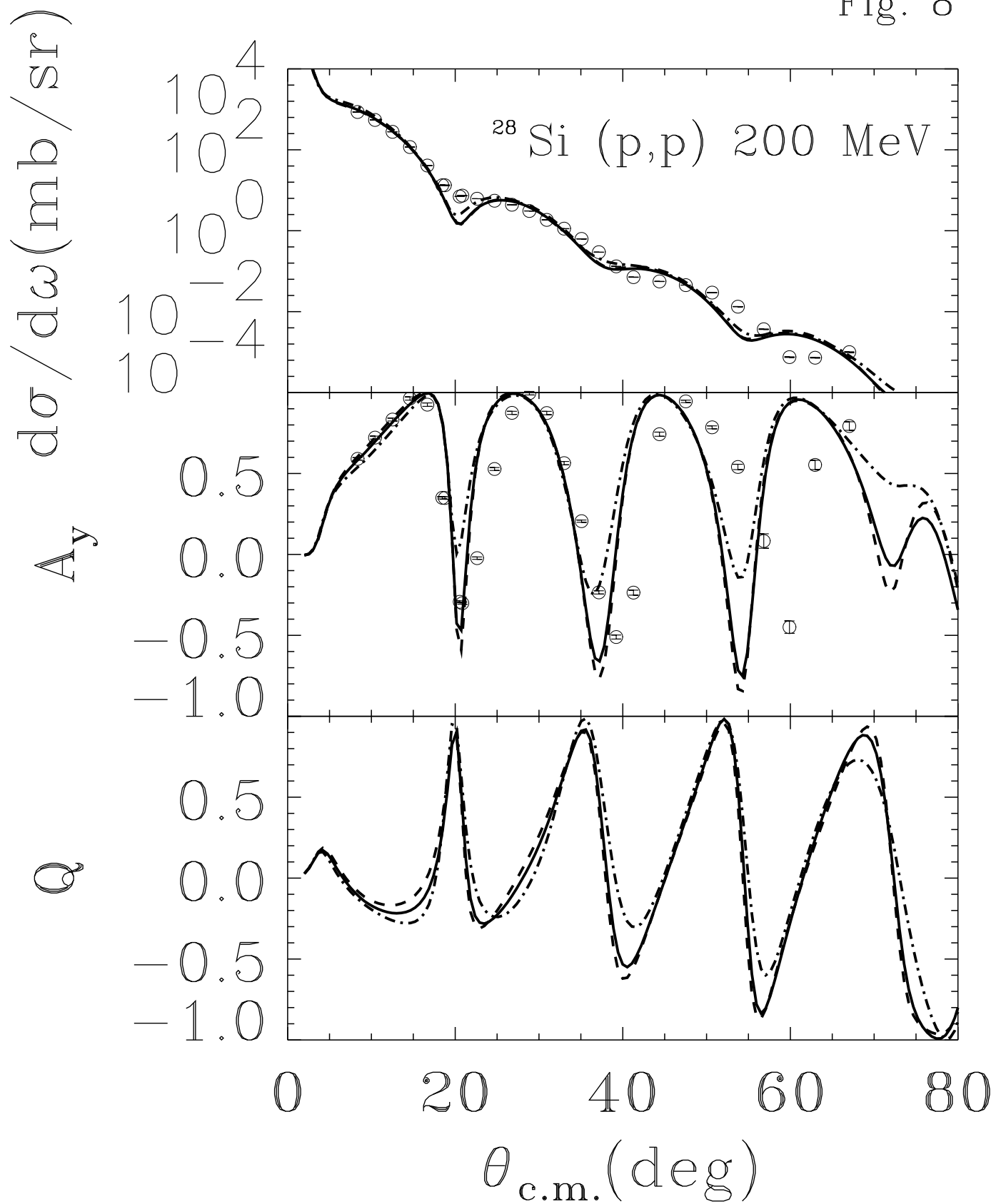


Fig. 9

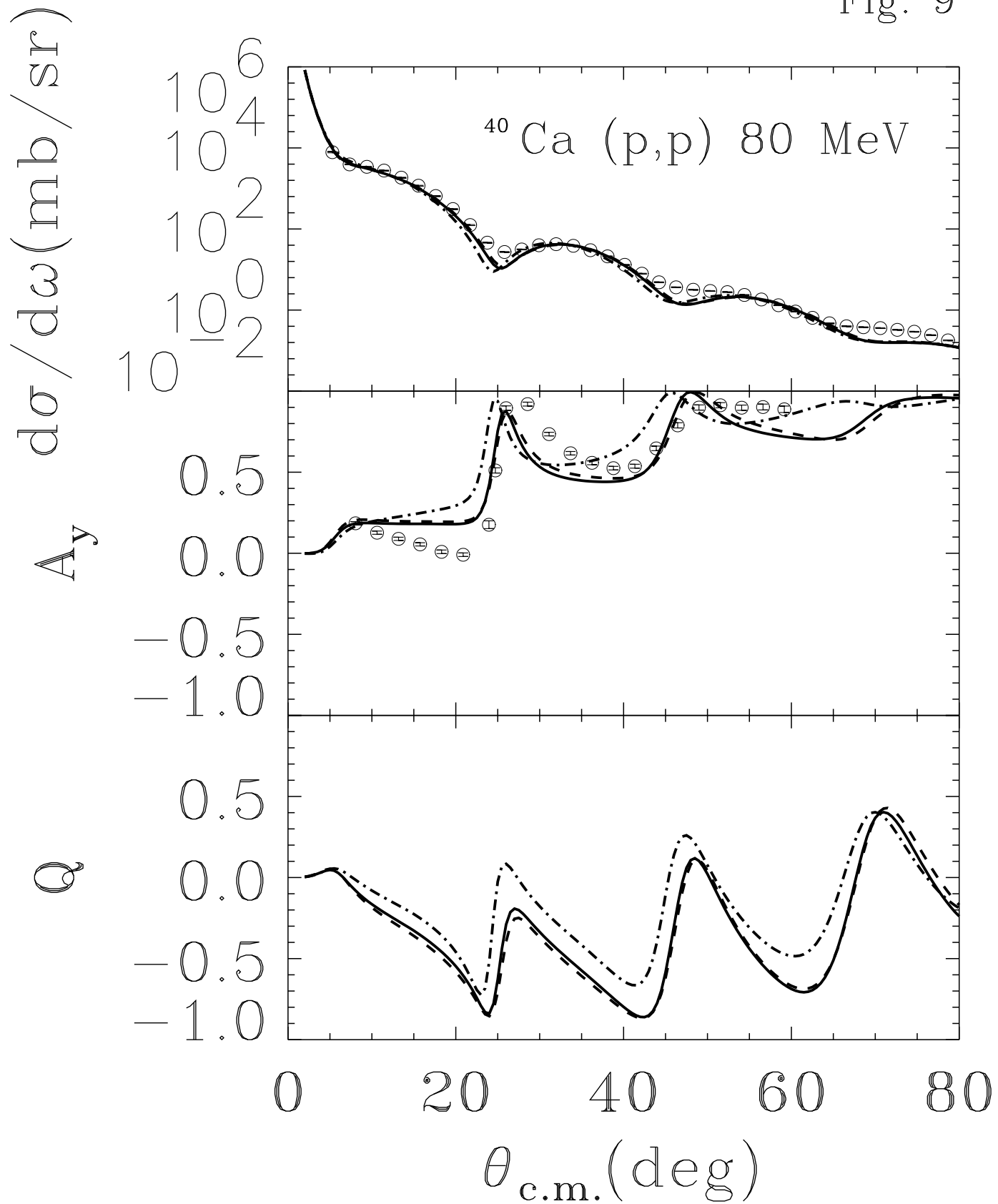


Fig. 10

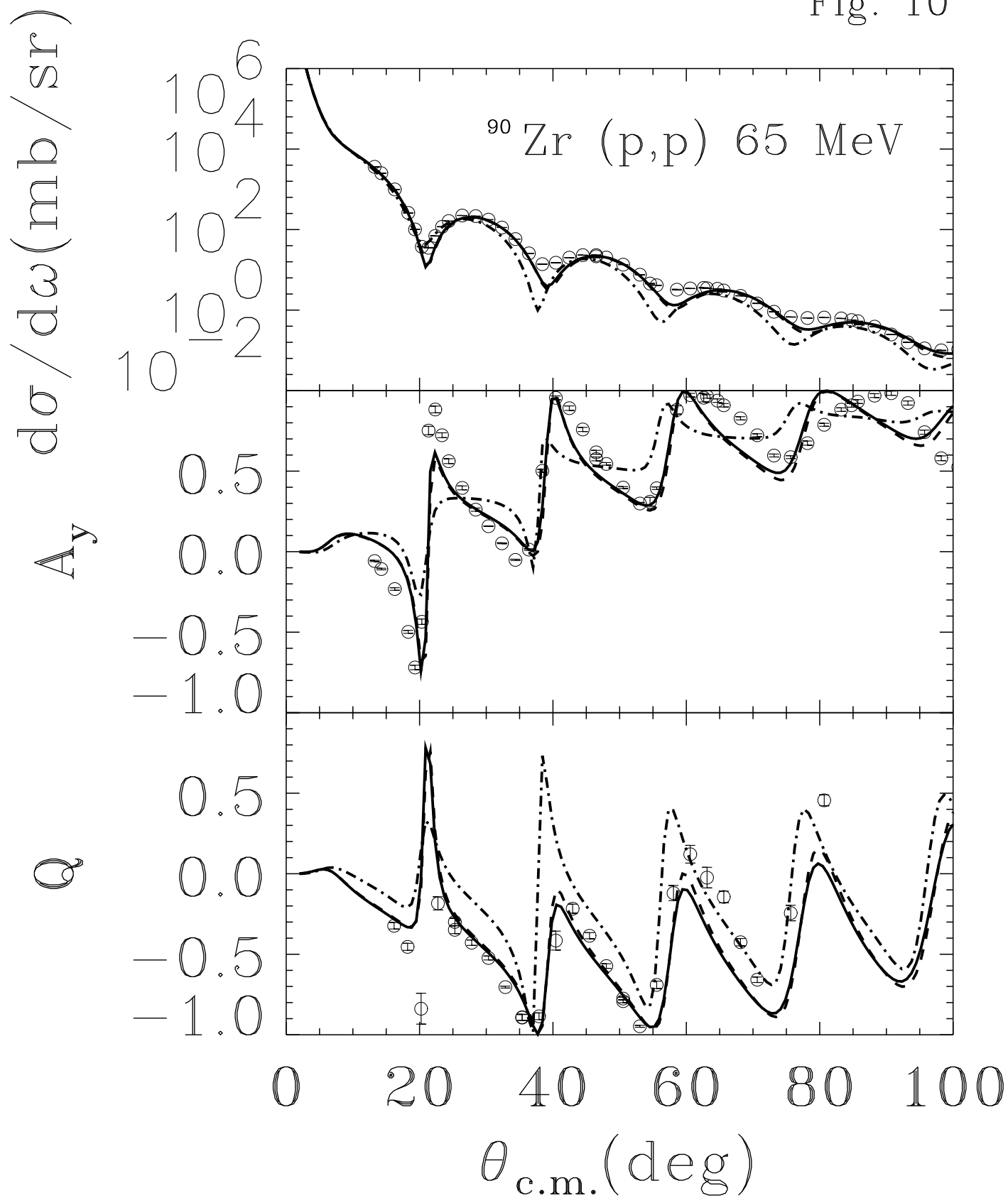


Fig. 11

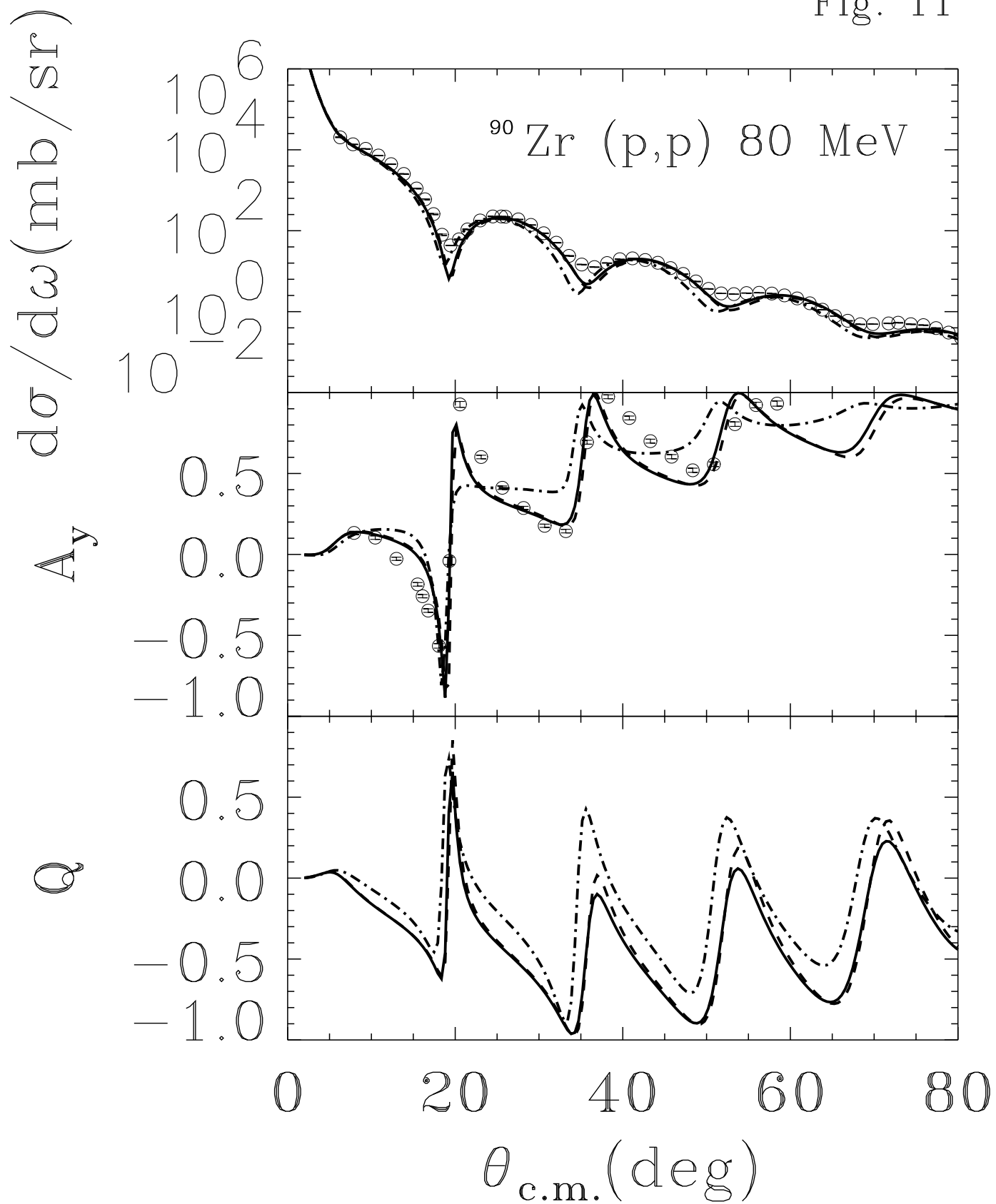


Fig. 12

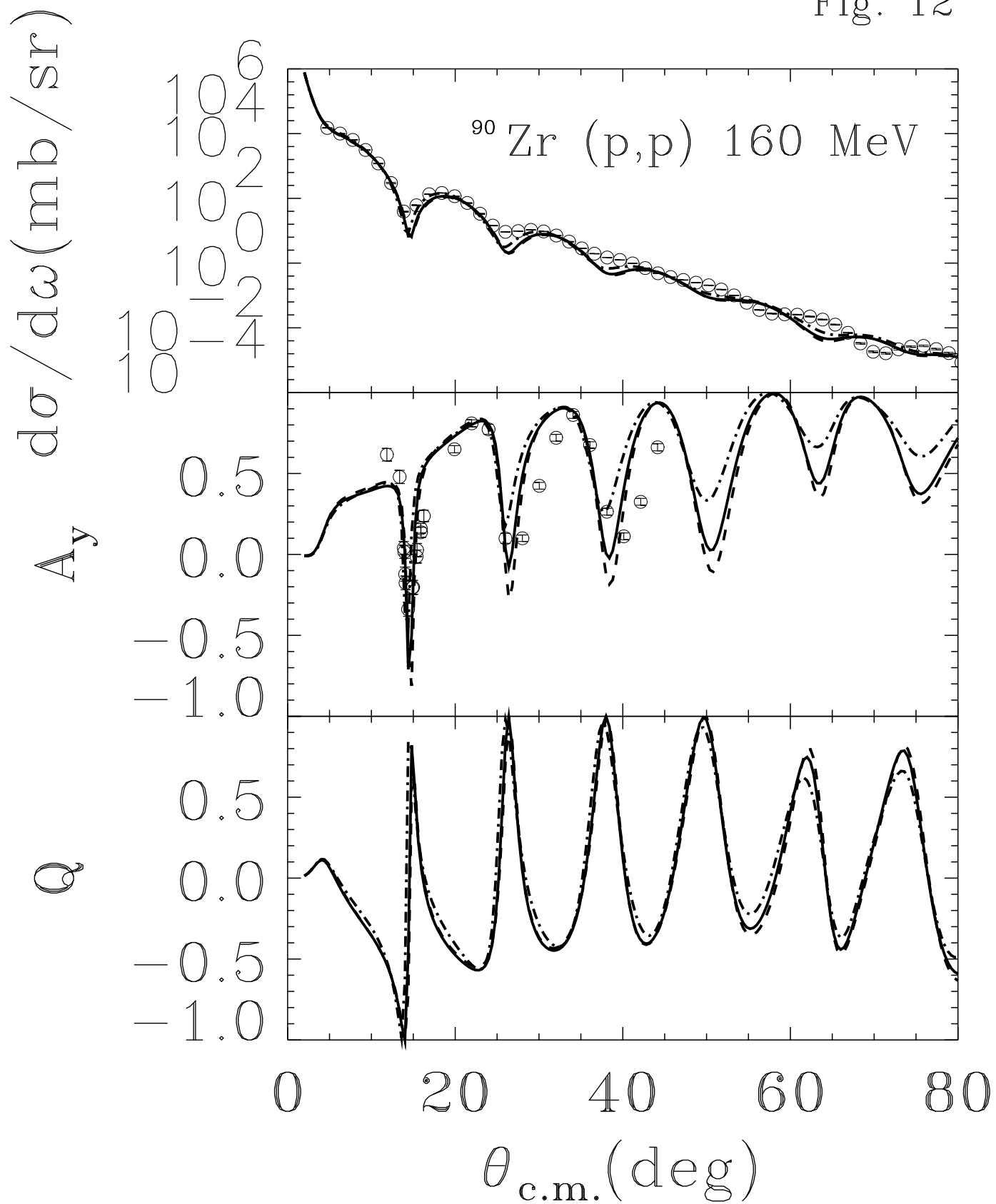


Fig. 13

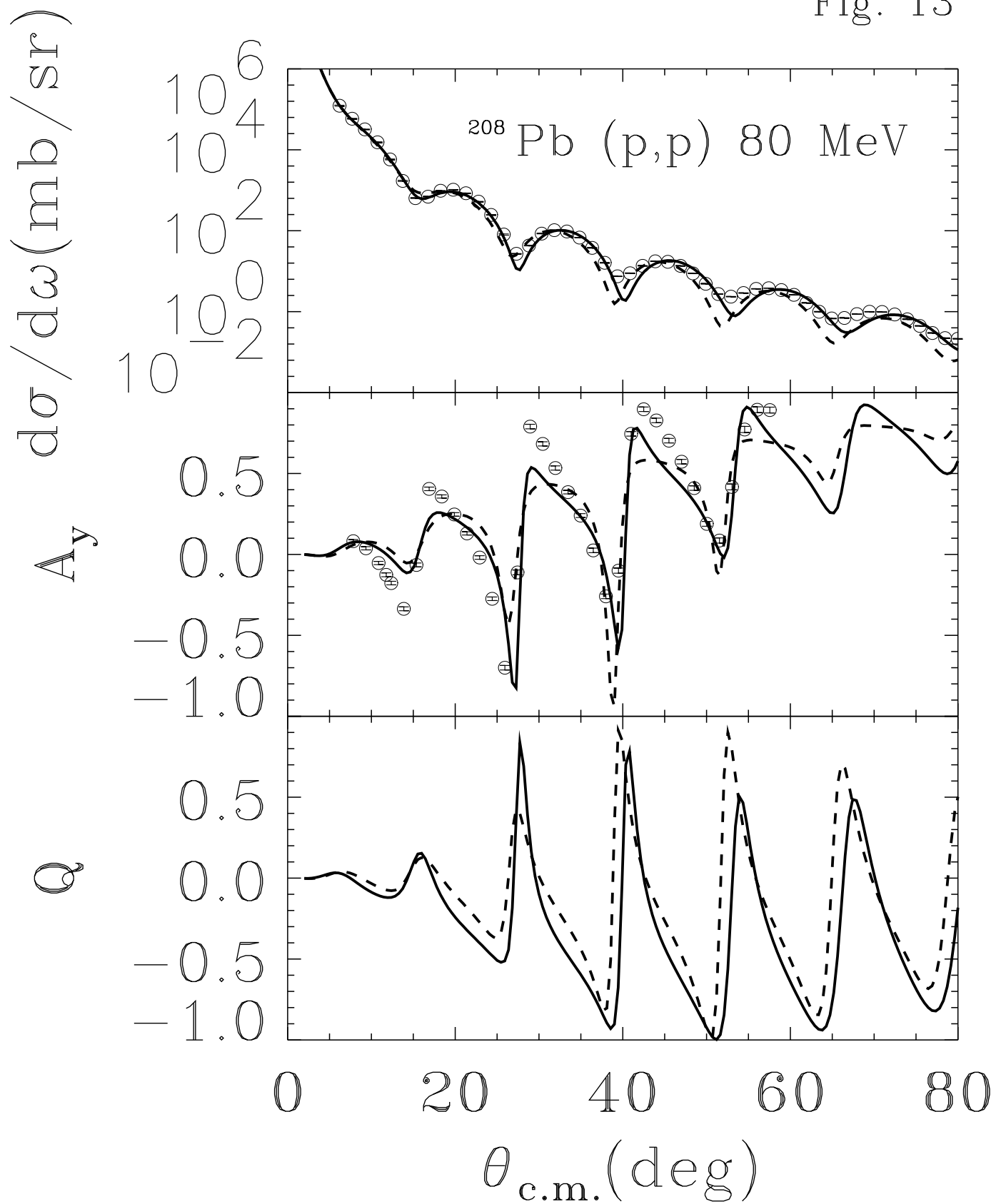


Fig. 14

